



# Synthesis of TiO(OH)2 precursor for low temperature sintering: A chemical and microstructural study

Lauriane Faure, Flora Molinari, Morgane Carfantan, Mario Maglione, Michaël Josse

## ► To cite this version:

Lauriane Faure, Flora Molinari, Morgane Carfantan, Mario Maglione, Michaël Josse. Synthesis of TiO(OH)2 precursor for low temperature sintering: A chemical and microstructural study. *Ceramics International*, 2023, 49 (17, Part A), pp.28337-28343. 10.1016/j.ceramint.2023.06.088 . hal-04151830

HAL Id: hal-04151830

<https://hal.science/hal-04151830>

Submitted on 5 Jul 2023

**HAL** is a multi-disciplinary open access archive for the deposit and dissemination of scientific research documents, whether they are published or not. The documents may come from teaching and research institutions in France or abroad, or from public or private research centers.

L'archive ouverte pluridisciplinaire **HAL**, est destinée au dépôt et à la diffusion de documents scientifiques de niveau recherche, publiés ou non, émanant des établissements d'enseignement et de recherche français ou étrangers, des laboratoires publics ou privés.

# Synthesis of $\text{TiO(OH)}_2$ precursor for low temperature sintering : a chemical and microstructural study

Lauriane Faure, Flora Molinari, Morgane Carfantan, Mario Maglione, Michaël Josse\*

\*michael.josse@icmcb.cnrs.fr

## **Abstract**

In this study, Titanium oxyhydroxyide powder was synthetized using a modified sol-gel route. This powder is widely studied as a catalyst for  $\text{CO}_2$  desorption but is here synthesized for the Cool-SPS sintering of titania based ceramics, as a reactive precursor. It is then important to maximize its reactivity at low temperature. The influence of different synthesis parameters (base used, temperature) on the final properties of the  $\text{TiO(OH)}_2$  powder is thus investigated. The final products were characterized by XRD, FTIR, SEM, granulometry and TGA. The microstructural parameters are crucial in order to obtain a satisfying reactivity for low temperature sintering and will determine the best parameters for the synthesis of  $\text{TiO(OH)}_2$ . Preliminary results concerning the sintering of  $\text{TiO}_2$  from this precursor are also reported.

**Key words :** Sol-Gel synthesis,  $\text{TiO(OH)}_2$ , reactivity, microstructure, Cool-SPS, Anatase Ceramic

## **1. Introduction**

Nowadays materials chemistry is increasingly turning towards the design of more sustainable materials and processes. Shaping processes, and especially sintering have made great steps in this direction during the past decade, with the emergence of low temperature sintering methods. Once H. Jantunen noticed how ceramic capacitors can be processed through “Room Temperature Fabrication” (RTF) [1] [2], other solvent-assisted sintering techniques re-emerged, such as the Cold Sintering Process [3], or hydrothermal sintering [4]. Since 2012 as well, Cool-SPS is being developed as a low temperature sintering technique. [5]–[7] From thermodynamically fragile ferroics to molecular ceramics [8], this solvent-free approach offers the opportunity to sinter materials that can not be shaped by conventional methods. To do so, this technique uses high pressures (up to 900MPa) and low temperatures (50 to 600°C) and can rely on specific precursors such as hydrates or hydroxides powders. [6], [7] Conversion of these

precursors to the target phase proved instrumental in obtaining both dense and cohesive ceramics of thermodynamically fragile materials. Indeed these chemicals are known to enhance the reactivity at low temperature as their decomposition temperature is low, and this strategy was also successfully applied to zirconia [9]. But one may go further using such precursors, for example by synthesizing a new phase at low temperature, from a mix of precursors, by reactive sintering. To do so, a good control of the precursors' characteristics is crucial.

In this study,  $\text{TiO(OH)}_2$  precursor synthesis is optimized in order to use it in the sintering of various titanate ceramics by Cool-SPS. This powder is widely used as a catalyst, for example for  $\text{CO}_2$  desorption. [10]–[12] It can also be used as a precursor for  $\text{TiO}_2$  synthesis. Here, the aim is to obtain a powder with small grain size, high specific surface and high reactivity that will be suitable for Cool-SPS sintering. The synthesis of this compound was detailed in a patent few years ago. [13] This synthesis can be described as a soft chemistry derivative of sol-gel synthesis in which a sol is formed by hydrolysis and condensation leading to the formation of a gel whose viscosity increases with time (maturation step). Nevertheless, this type of synthesis is generally carried out starting from molecular precursors such as metal alkoxides of formula  $\text{M(OR)}_n$  where M is a metal having a degree of oxidation n and OR a deprotonated alcohol, which is not the case in our work. Indeed, the precursor  $\text{TiOSO}_4 \cdot x\text{H}_2\text{O} \cdot x\text{H}_2\text{SO}_4$  was chosen, which is an intermediate in ore treatment, contrary to the titanium alkoxide, which is the compound used in the patent and requires multiple synthesis steps, thus increasing its cost, from financial as well as environmental standpoint.

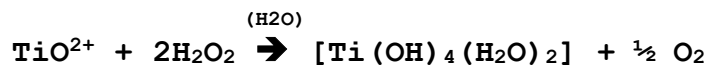
Different synthesis parameters were explored, such as the base used and the reaction temperature, and the precursors subsequently obtained were then characterized by XRD to check their structural properties, while the presence of residual chemicals was also tested by FTIR. Laser granulometry analyses were performed to study the particle size which can influence the reactivity. The microstructures of the particles were also checked by SEM. Finally the reactivity of this precursor was evaluated by TGA, and preliminary sintering experiments were conducted to obtain  $\text{TiO}_2$  ceramics by Cool-SPS.

## 2. Materials and methods

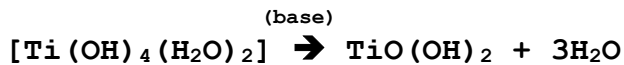
### 2.1. Synthesis

The synthesis was reproduced using the same method as described in the patent but using a different starting compound. The Titania precursor was synthetized using  $\text{TiOSO}_4 \cdot x\text{H}_2\text{O} \cdot x\text{H}_2\text{SO}_4$  commercial powder as a starting compound (*Titanium (IV) oxide sulfate*

*sulfuric acid hydrate, Alfa Aesar*). The aim of the synthesis is to obtain titania oxyhydroxide  $\text{TiO(OH)}_2$ . The Titania oxide sulfate was partially dissolved in distilled water. Hydrogen peroxide was added to the  $\text{TiOSO}_4 \cdot x\text{H}_2\text{O} \cdot x\text{H}_2\text{SO}_4$  in a second time for the hydrolysis of the compound. Considering that the selected precursor is known to yield titanyl ions ( $\text{TiO}^{2+}$ ) in solution, the reaction can be described as follows :



After this step, a strong base can be added, usually sodium hydroxide ( $\text{NaOH}$ ) or ammonium hydroxide ( $\text{NH}_4\text{OH}$ ). These basic solutions are very common and represent a limited cost. The addition of a strong base leads to an exothermic reaction and aims at neutralizing the sulfate group present in the starting precursor as well as the condensation of the complexes  $[\text{Ti(OH)}_4(\text{H}_2\text{O})_2]$  into  $\text{TiO(OH)}_2$ . This second reaction can be described as follows :



As the starting precursor is an oxysulfate compound, using a strong base such as  $\text{AOH}$  (with  $\text{A} = \text{Na}$  or  $\text{NH}_4$ ) leads to the obtention of sulfates  $\text{A}_2\text{SO}_4$  in the solution which are eliminated by washing. The solution has to rest for few hours before the formation of a yellow precipitate can be observed, which is then washed with distilled water before being dried at  $50^\circ\text{C}$ .

It was shown in the initial study that different bases could be used for the synthesis, and that the maximum synthesis temperature is  $90^\circ\text{C}$ . From there, it was decided to investigate which synthesis parameters would allow to produce a powder suitable for Cool-SPS purposes.

The first parameter studied is the modification of the base solution used. Two different routes were tested: ammonium hydroxide and sodium hydroxide. Depending on the basic route, different morphologies of grains can be obtained. In a second time the synthesis temperature was changed, it is specified in the patent that the synthesis could be done up to  $90^\circ\text{C}$  maximum because at a higher temperature, the product is not homogeneous, and the particle diameters will increase. Then, three different temperatures were studied:  $20^\circ\text{C}$  (room temperature), a low temperature synthesis ( $5^\circ\text{C}$ ) and a higher temperature synthesis ( $50^\circ\text{C}$ ). As small particles are needed, the maximum temperature explored was not higher than  $50^\circ\text{C}$  and the aforementioned patent also reported that above  $50^\circ\text{C}$  the grain size will increase and the final phase  $\text{TiO(OH)}_2$  may not be obtained pure.

## **2.2. Characterization**

X-ray diffractions analysis were performed on the obtained powders to examine their crystallinity and confirm the absence of any residual crystalline phase. The data was collected at room temperature with a PANalatycal, X'pert pro MPD diffractometer using a Cu K $\alpha$  radiation ( $\lambda K_{\alpha 1} = 1.5406 \text{ \AA}$  and  $\lambda K_{\alpha 2} = 1.5444 \text{ \AA}$ ) The geometry used was Bragg Brentano and the range of data collection 2 theta was between  $8^\circ$  and  $80^\circ$  with a step size of  $0.02^\circ$ .

Variable Temperature X-ray diffractions analysis (VT-XRD) data was collected with a PANalatycal, X'pert MPD diffractometer (using a Cu K $\alpha$  radiation) with Bragg-Brentano geometry equipped with a graphite back monochromator and an Anton-Paar HTK16 chamber.

FTIR measurements were carried on powder samples using an Equinox 55 Bruker spectrometer. The measurements were performed using diffuse reflectance set up in a range of  $4000$  to  $400\text{cm}^{-1}$ . Each sample was mixed with Potassium Bromide KBr for calibration.

Scanning Electron Microscopy (SEM) observations were made on different powders. The samples were metallized using a gold sputtering apparatus. The images were taken using the JSM-6360A-JEOL microscope with Energy Dispersive spectroscopy probe. Pictures were collected with secondary and backscattered electrons.

Granulometry measurements were made using a MASTER SIZER 2000 laser granulometer (with a wavelength of  $633\text{nm}$ ). All samples were measured by liquid route method using distilled water as a solvent. Ultrasounds were applied on the solution before measuring in order to break most of the agglomerates and measure precise D10, D50 and D90 for each sample. They represent the diameters for which 10%, 50% and 90% (in volume) of the sample's particles have a diameter smaller than D10, D50 or D90 respectively.

TGA analyses were conducted on different powder samples. This measurement was performed using a TA Instruments device (TGA Q50), under air from room temperature to  $1000^\circ\text{C}$  (one hour dwell time) with heating and cooling rates of  $3^\circ\text{C}/\text{min}$ .

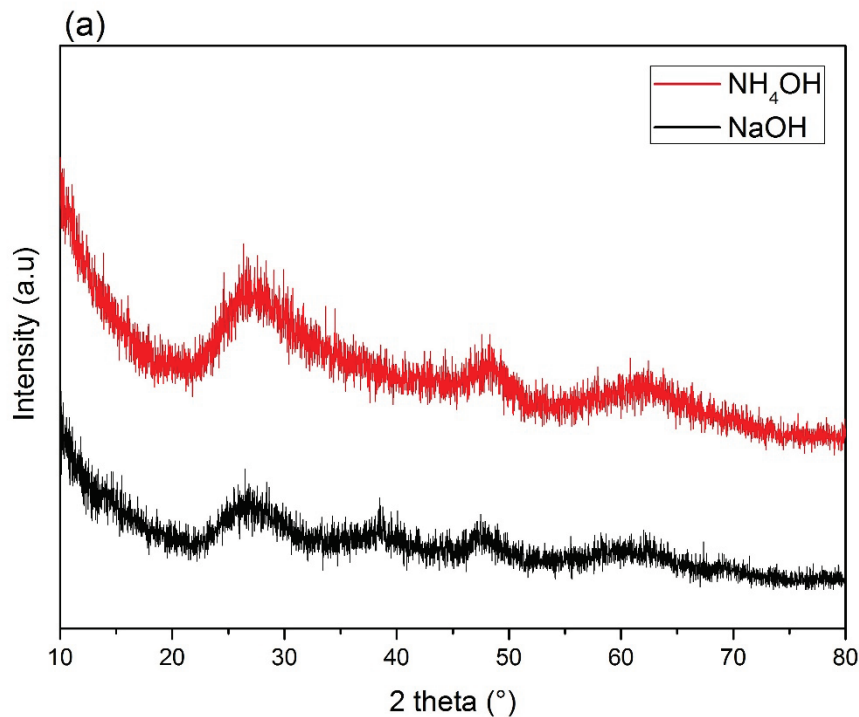
## **3. Results and discussion**

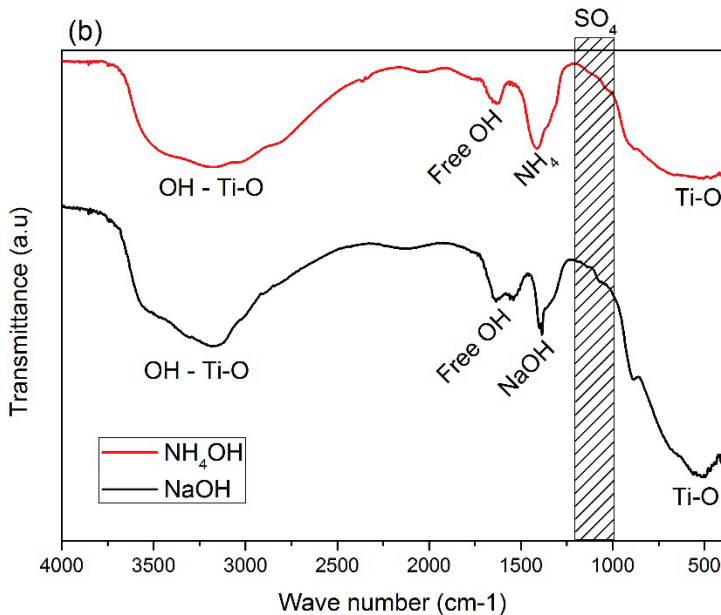
### **3.1. Modification of the base used**

The first parameter studied was the modification of the base reacting with the titanium complex during the second step of the synthesis. Two strong bases were chosen, ammonium hydroxide and sodium hydroxide, with respective pH of 13.1 and 11.6.

In the case of the sodium hydroxide synthesis, the reaction is strongly exothermic as compared to the ammonium hydroxide synthesis, due to the difference in pH. Thus, differences in composition and microstructures are expected, and are even visible macroscopically, with larger grains in the sodium hydroxide synthesis, compared to those obtained through ammonium hydroxide synthesis. This is then confirmed after the washing and drying steps of both syntheses. Indeed, the powder in the ammonium hydroxide route is very fine and volatile whereas in the case of the sodium hydroxide route, small transparent orange crystals are obtained.

After drying, the powders resulting from the synthesis of sodium hydroxide and ammonium hydroxide are crushed in a mortar. The powders are first analyzed by XRD and FTIR in order to compare their crystallinity and identify the chemical groups present. (Fig.1).



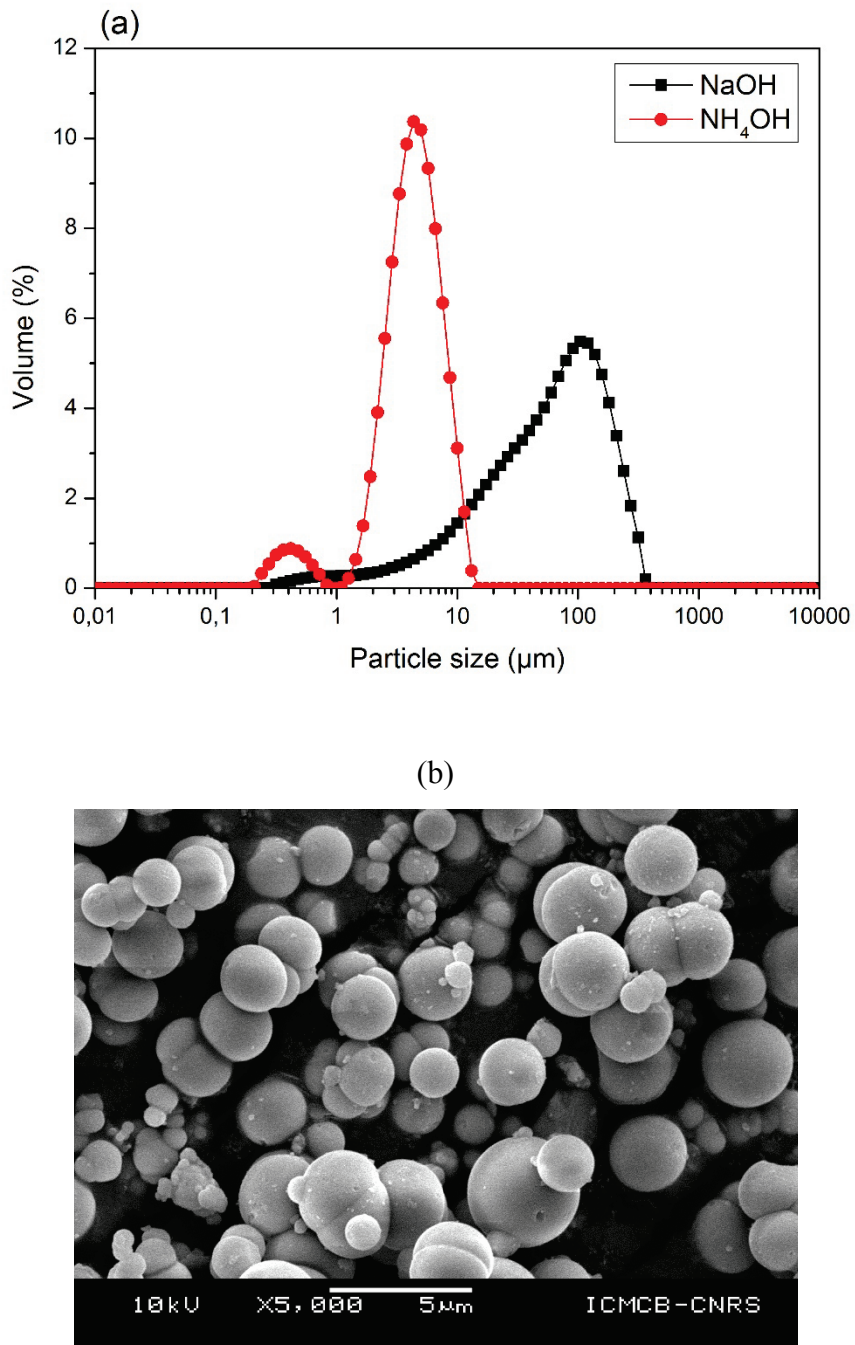


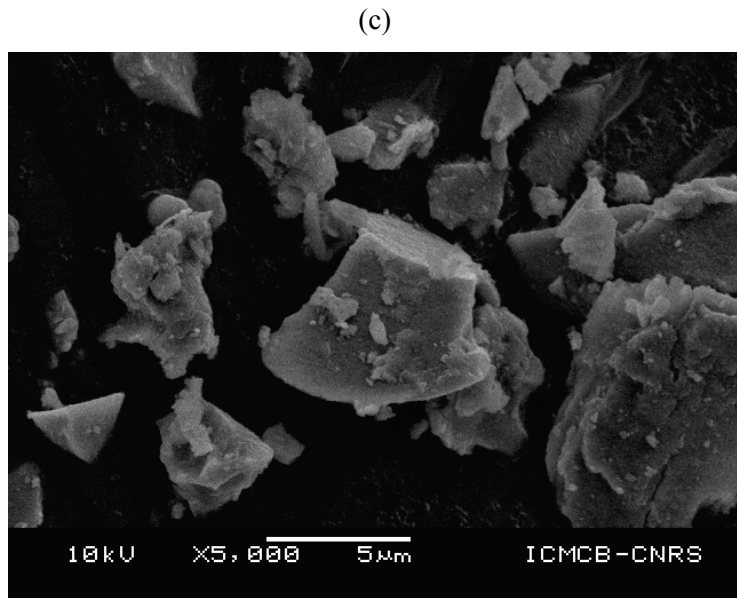
*Figure 1: (a) XRD patterns obtained on  $\text{TiO}(\text{OH})_2$  precursor synthetized by ammonium hydroxide and sodium hydroxide routes. (b) corresponding FTIR data.*

Fig.1 (a), shows that both powders display very low crystallinity corresponding to the literature data. [12] In the case of the sodium hydroxide synthesis, an additional signal appears to be present around  $38^\circ$  and is not visible in the diffractogram of the ammonium hydroxide route. Due to the very weak crystallinity, it is difficult to index these peaks and determine with certainty which compound is responsible for this extra contribution. For that, the FTIR analysis allows to complete the result. (Fig.1 (b)).

On both curves, the presence of Ti-O bond is very clear as well as the signature of OH groups bound to Ti-O. The signature of free OH groups is also visible and represents the water in the compound. The signature of our precursors is in good agreement with the literature data of the pure  $\text{TiO}(\text{OH})_2$  compound. [14] In addition,  $\text{NH}_4^+$  groups and the signature of NaOH are visible in the two syntheses respectively in ammonium and sodium hydroxide routes. In spite of repeated washes, these groups are still present. This is likely due to the residual sodium hydroxide being strongly bound to titanium precursor particles. Moreover, there is a risk of dissolving the titania hydroxide precipitate formed, with repeated washing. For the sake of yield and to limit synthesis complexity, it is not sought to remove all sodium or ammonium hydroxide from the final powder. An important point from FTIR spectra is the absence of sulfates, as highlighted in Fig.1 (b), as their presence could be expected from the starting material (acidic titanium oxysulfate).

From a grain size and microstructure point of view, the two syntheses present large differences that were quantified by particle size analysis and observed by SEM imaging. (Fig.2)





*Figure 2: (a) granulometry analysis obtained on  $TiO(OH)_2$  precursor synthetized by ammonium hydroxide and sodium hydroxide routes. (b) and (c) corresponding SEM Images for respectively ammonium hydroxide and sodium hydroxide routes.*

The two syntheses show very different characteristics of size and microstructure. The red curve (NH<sub>4</sub>OH synthesis), shows a bimodal behavior, which is a very good characteristic of the powder as this type of distribution facilitates the sintering process. In the case of the black curve (NaOH synthesis), the distribution is trimodal, but the particles are larger than in the ammonium hydroxide synthesis. There is significant size heterogeneity in this sample.

On the particle size analysis, in the case of the ammonium hydroxide synthesis, the D<sub>50</sub> is 4.61 $\mu$ m against 67.61 $\mu$ m for the sodium hydroxide synthesis (Fig.2 (a)). This very large difference is explained by the much more exothermic synthesis reaction in the case of sodium hydroxide route, necessarily leading to a growth of grains more important than for the ammonium hydroxide way. The particle size analysis is confirmed by SEM imaging observations performed on these powders. (Fig.2 (b,c)). The morphologies are very different from one synthesis to another. Indeed, in the case of the ammonium hydroxide synthesis, the grains are spherical of relatively homogeneous size. The granulometric analysis shows a size distribution ranging from D<sub>10</sub>=2.12 $\mu$ m to D<sub>90</sub>=8.68 $\mu$ m. This morphology is the preferred morphology for efficient sintering. However, in the case of sodium hydroxide synthesis, the grains exhibits flat surfaces and very variable sizes. The size distribution here is between D<sub>10</sub>=8.76 $\mu$ m to D<sub>90</sub>=202.67 $\mu$ m. These granulometric characteristics are nonetheless "apparent" because the powder presents aggregates that sonication fails to break. Indeed the

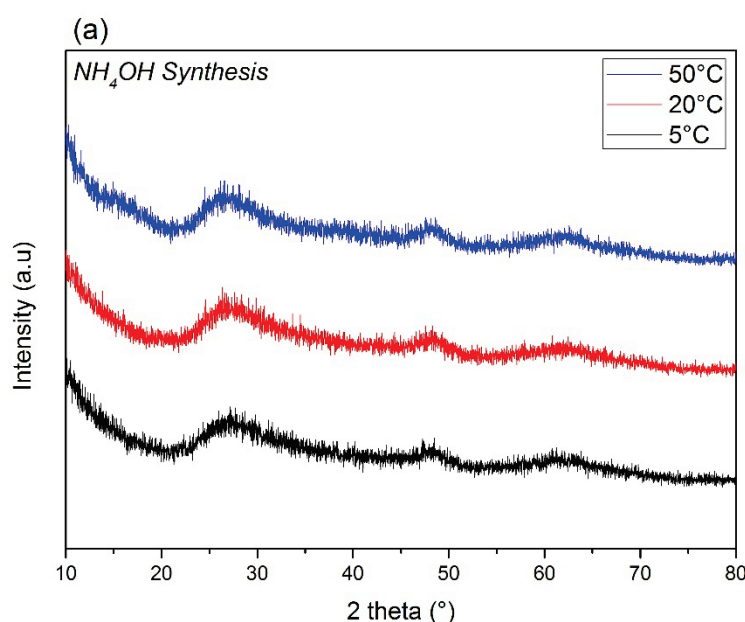
SEM imaging suggests that the grains are made of very fine crystallites, which could not be observed in our experimental conditions.

### ***3.2. Variation of the synthesis temperature***

Considering the great differences in microstructures related to the use of sodium hydroxide, more exothermic than ammonium hydroxide, the question of the influence of the synthesis temperature arose. In the patent and in various studies, it is specified that the  $\text{TiO(OH)}_2$  phase can be synthesized in a temperature range from ambient to 100°C. However, the microstructure of the final powder is very important for Cool-SPS sintering and therefore it is necessary to determine the influence of the synthesis temperature. This temperature can vary slightly depending on the weather conditions.

Thus, three syntheses were carried out at 5°C, 20°C and 50°C. For the synthesis at 5°C, the objective is to determine if finer particles can be obtained at lower temperature, while remaining above 0°C, keeping a simple (ice immersion setup) and cheap experimental process. For 50°C, the aim was to check the influence of temperature on particle growth, and a hot plate was used. The reactive solutions (Hydrogen peroxide and basic solutions) were not cooled or heated before being introduced into the reaction mixture in order not to denature their chemical composition.

XRD analyses were first performed on the three powders obtained at 5°C, 20°C and 50°C. (Fig.3)



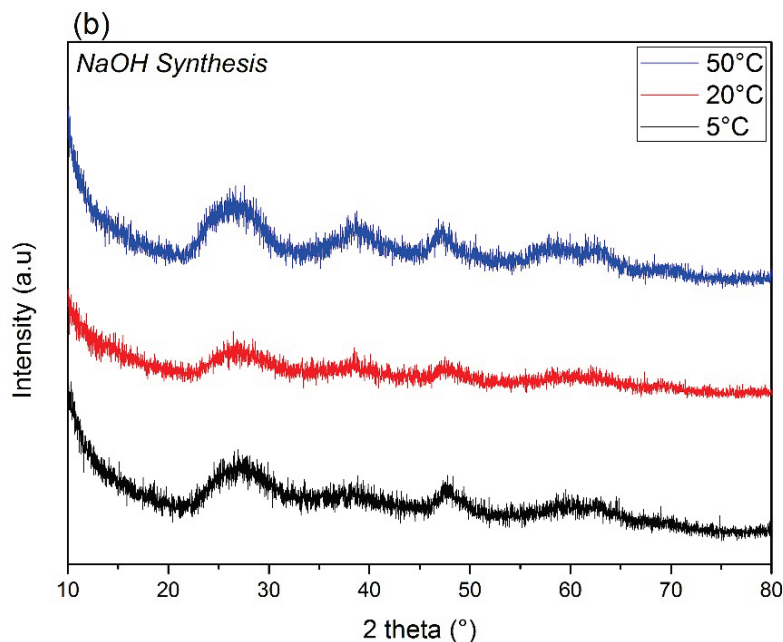


*Figure 3: (a) XRD patterns obtained on  $TiO(OH)_2$  precursor synthetized by ammonium hydroxide at different temperatures.  
(b) XRD patterns obtained on  $TiO(OH)_2$  precursor synthetized by sodium hydroxide route at different temperatures.*

In the case of ammonium hydroxide route (Fig.3 (a)), no significant difference is visible on the XRD patterns. There is no secondary crystallized phase, which means that the chemical composition is not modified with temperature. From a chemical point of view, the synthesis in the case of sodium hydroxide route, does not seem to evolve according to the temperature. Only a slight increase of the crystallinity is visible (in the case of the synthesis carried out at 50°C) on the peak present at 38°.

Concerning grain size and morphology, granulometric analysis (Fig.4 (a,b)) and SEM imaging (Fig.5 (a,b,c,d,e,f)) were performed.

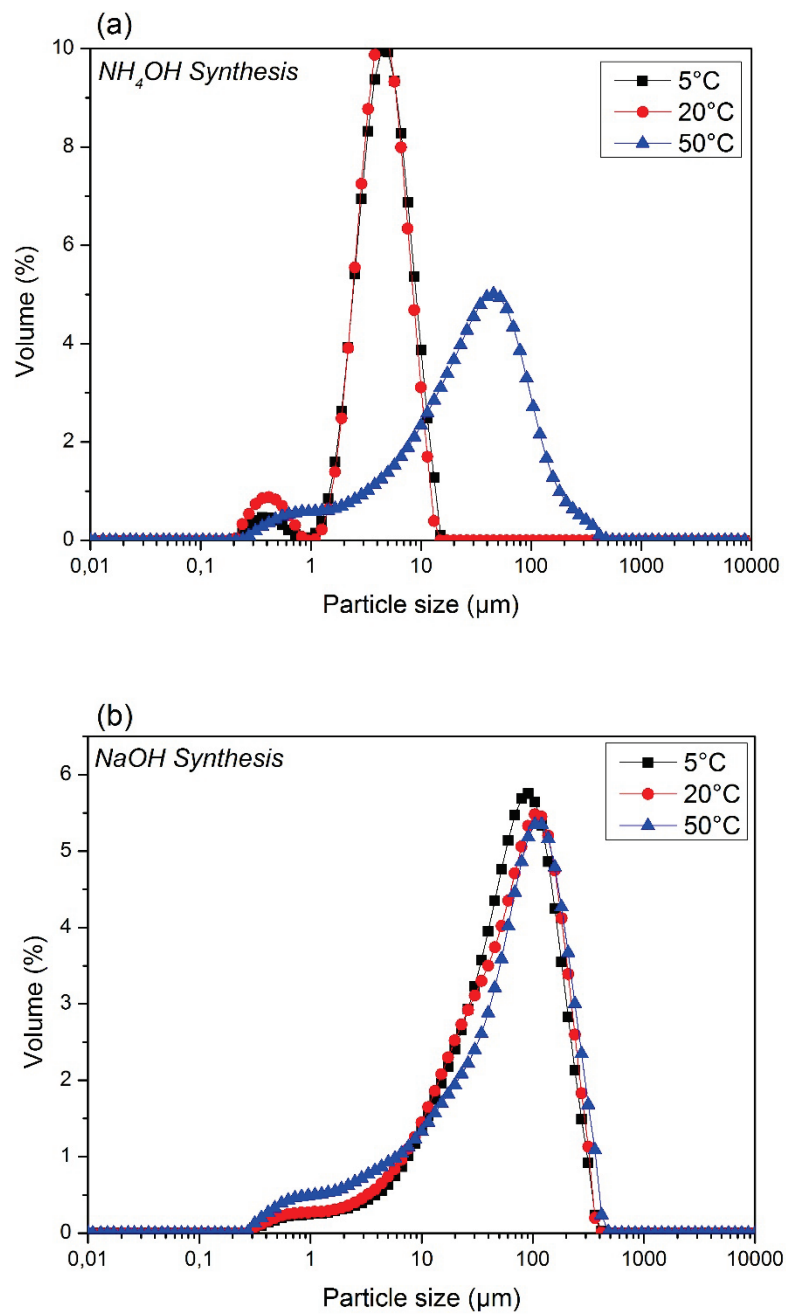


*Figure 4: (a) granulometry analysis obtained on  $TiO(OH)_2$  precursor synthetized by ammonium hydroxide at different temperatures. (b) granulometry analysis obtained obtained on  $TiO(OH)_2$  precursor synthetized by sodium hydroxide route at different temperatures.*

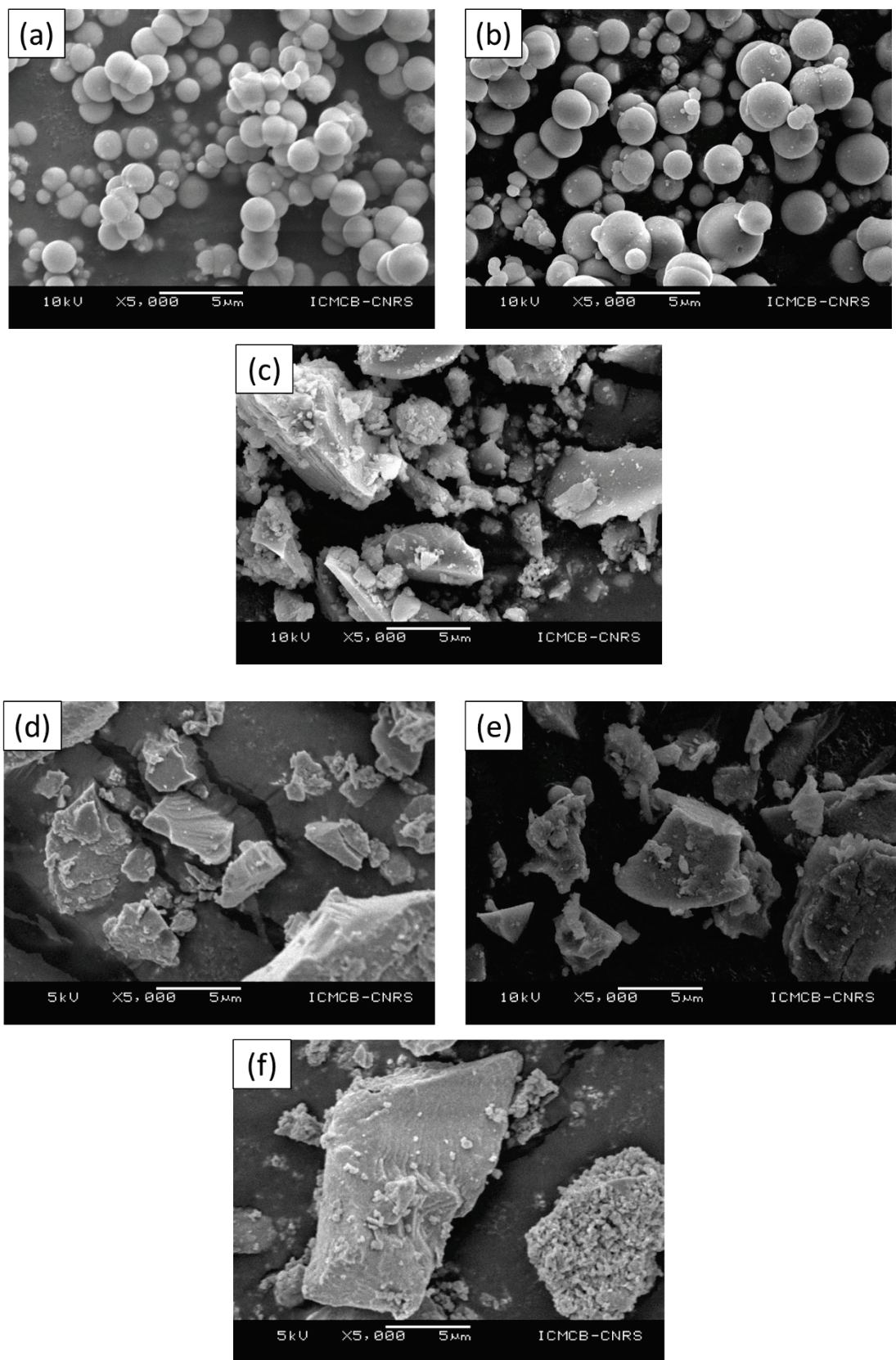


*Figure 5: (a,b,c) SEM pictures taken on  $TiO(OH)_2$  precursor synthetized by ammonium hydroxide at respectively 5°C, 20°C and 50°C. (d,e,f) SEM pictures taken on  $TiO(OH)_2$  precursor synthetized by sodium hydroxide at at respectively 5°C, 20°C and 50°C.*

Fig.4 (b) shows that the distribution and the size of the grains from the sodium hydroxide route do not seem to be affected by the increase of the synthesis temperature because the grain size curves are almost stackable. The microstructure is very similar regardless of the synthesis temperature is (Fig.5 (d,e,f)). These experiments show that in the case of this sodium hydroxide route, the temperature of the reaction medium has little importance compared to the temperature locally generated by the exothermic reaction occurring.

In the case of ammonium hydroxide route, at 5°C and at 20°C, the particles are almost similar in size with an almost stackable bimodal distribution (Fig.4 (a)). The synthesis at 5°C has a D<sub>50</sub> of 4.84µm and that at room temperature has a D<sub>50</sub> of 4.61µm. However, at 50°C, an important grain growth is visible, with D<sub>50</sub> reaching 32.16µm. It is confirmed with the SEM images where large faceted grains are observable (Fig.5 (a,b,c)). This morphology is similar to the one observed on the grains from the sodium hydroxide synthesis, which confirms that the grain growth occurring is thermally activated.

In the case of the sodium hydroxide synthesis, it is activated by the exothermic reaction between NaOH and the titanium complexes, and in the case of the ammonium hydroxide synthesis, it is simply activated by the temperature. It is thus preferable in the framework of this work not to exceed the room temperature for this synthesis, while cooling to 5°C is not necessary, the aim being to keep small particles and a spherical morphology.

### ***3.3. Stability and reactivity of the precursor***

In the continuity of the study of the synthesis of the titanium precursor, it is important to know its behavior with respect to temperature. The TGA analysis gives valuable information on the typical decomposition temperatures of the compound. (Fig.6)

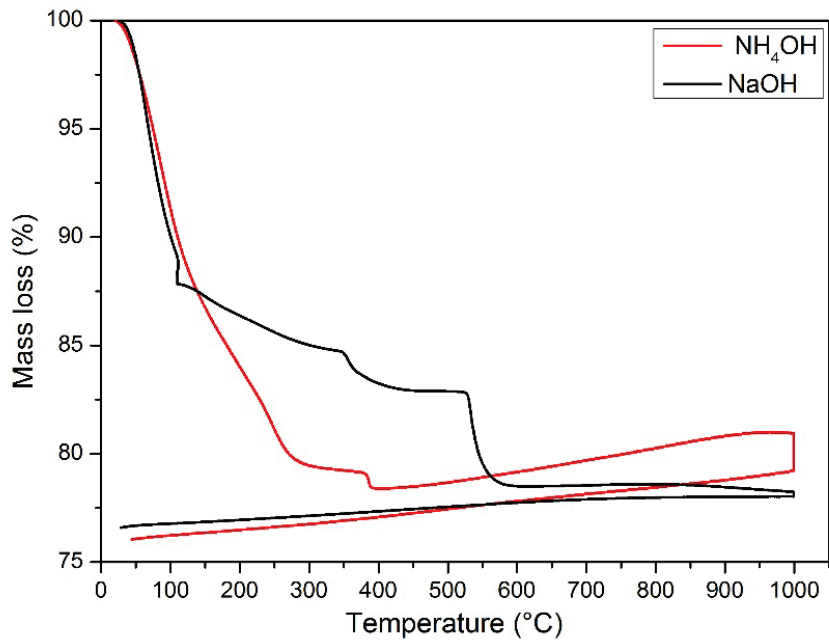


Figure 6: TGA analysis on sodium hydroxide and ammonium hydroxide precursors.

Upon conversion into  $\text{TiO}_2$ , titatnium oxyhydroxide  $\text{TiO(OH)}_2$  releases one water molecule, which represents a mass loss of around 18,4%. As can be expected from a room temperature synthesis in solution, the powders may encompass extra water molecules. Indeed in the case of the ammonium hydroxide synthesis, a significant mass loss of 20% occurs between room temperature and 250°C. This loss probably corresponds to the departure of the free and bound water present in the precursor. The visible stall at 350°C likely corresponds to the final step of the conversion of the precursor into  $\text{TiO}_2$ . This means that the precursor is highly reactive at low temperature and thus shows an advantage for Cool-SPS sintering. Instead, in the case of sodium hydroxide synthesis, various phenomena occur and persist at higher temperatures, and a mass loss beyond 18% is not reached until 550°C. The first mass loss (from room temperature to 100°C) corresponds again to a departure of free water, the second likely to some bound water (from 120°C). Again, a stall around 350°C is visible and may correspond to further dehydroxylation associated with the decomposition of the precursor. Nevertheless, a sudden loss of mass is visible at 550°C; this is probably the complete decomposition of the precursor. In the case of this synthesis route, the reactions continue until about 600°C, which is too high, compared to the ammonium hydroxide route, for our subsequent reactive sintering application.

To complete the investigation of  $\text{TiO(OH)}_2$  precursor synthesized by ammonium hydroxide route, a variable temperature XRD (VT-XRD) study was conducted under air. (Fig.7)

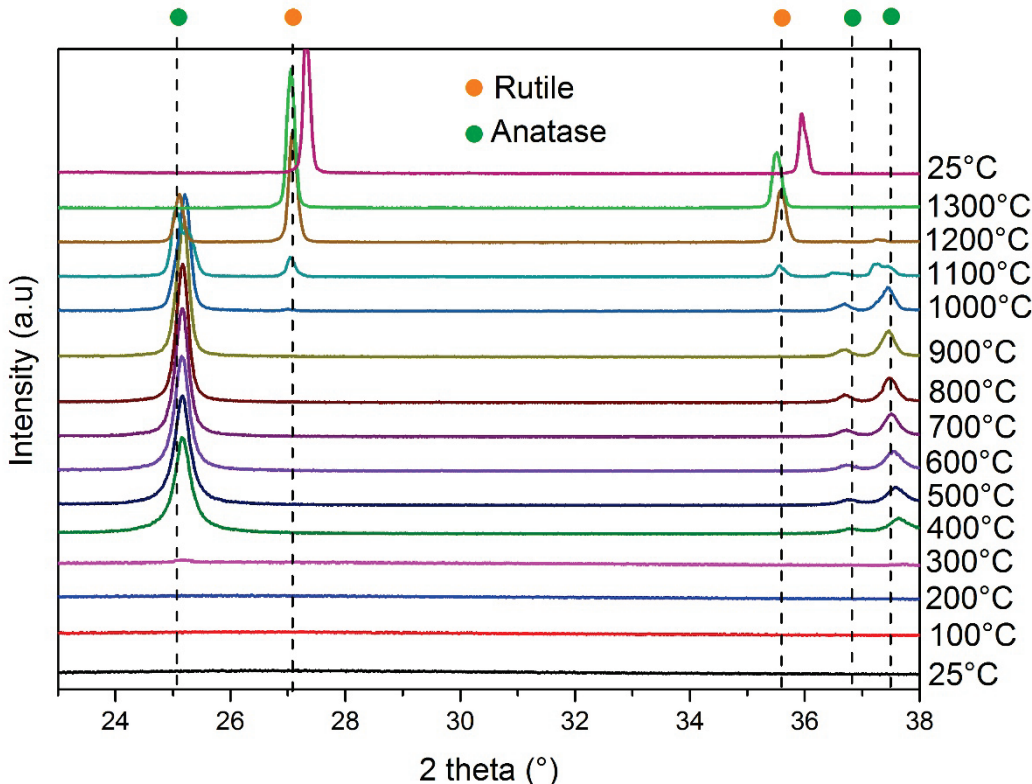


Figure 7: VT-RXD performed on ammonium hydroxide route precursor

VT-XRD data confirms the formation of  $\text{TiO}_2$ , in the anatase form, between  $300^\circ\text{C}$  and  $400^\circ\text{C}$  (the sample remaining amorphous at lower temperatures). It also suggests that the stall observed around  $350^\circ\text{C}$  in TGA data correspond to crystallization of anatase, forcing the release of residual water. Note that the top pattern was collected at room temperature, after cooling the system from  $1300^\circ\text{C}$ . The shift is due to thermal contraction.

Surprisingly, the anatase structure is retained beyond  $1000^\circ\text{C}$ , and until at least  $1200^\circ\text{C}$ . The rutile phase appears at  $1100^\circ\text{C}$  and is the only phase present at higher temperatures. It should be recalled that the anatase-rutile transition is expected around  $700^\circ\text{C}$  [15]. Thus beyond providing low-temperature reactivity for Cool-SPS, the  $\text{TiO(OH)}_2$  precursor prepared via the ammonium hydroxide route favors the stabilization of the anatase phase well beyond its known thermal stability region (from  $700$  to  $1100^\circ\text{C}$ ). This is a remarkable benefit, as anatase-structured  $\text{TiO}_2$  receives a large scientific and technological interest, for example in light-driven application (catalysis, energy conversion...).

In order to confirm the suitability of this precursor for low temperature sintering, preliminary Cool-SPS attempts have been run using  $\text{TiO}(\text{OH})_2$  to elaborate  $\text{TiO}_2$  ceramics. When using a 300 MPa pressure at 600°C, a phase pure  $\text{TiO}_2$  ceramic was recovered as illustrated by Fig.8. It is also remarkable that following sintering under pressure, the Anatase structure is retained, as pressure usually favors the denser phase, which is Rutile ( $4.250\text{g.cm}^{-3}$ , vs  $3.983\text{g.cm}^{-3}$  for Anatase). However it should be recalled that Anatase stability can be extended to a similar temperature range when synthesized through a modified sol-gel method. [16]

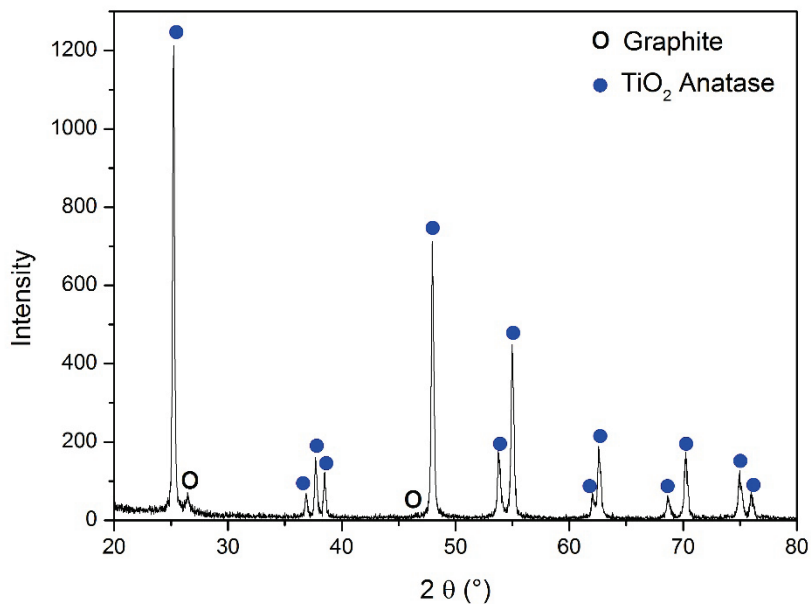


Figure 8: XRD analysis obtained on a  $\text{TiO}_2$  ceramic sintered using the ammonium hydroxide route precursor.

The relative density of the ceramic (as determined by geometrical measurement) is  $86\pm2\%$ , which is quite good for an unoptimized preliminary experiment. Further experiments on the preparation of  $\text{TiO}_2$  ceramics will be conducted and reported elsewhere in the near future, as these preliminary results are only reported for illustrative purpose concerning the synthesis of the  $\text{TiO}(\text{OH})_2$  precursor.

In addition,  $\text{TiO}_2$  ceramics processed from the Na-route precursor can be obtained, however their quality is hampered by spurious reactions related to remaining Na traces.

## **4. Conclusion**

In this study, the titanium compound  $\text{TiO(OH)}_2$ , was synthetized using a sol-gel derived synthesis route. This method involves a titanium-based starting material which composition is close to that of the extraction ore, as well as very simple reactants such as strong bases and hydrogen peroxide. Experiments on the variation of the synthesis parameters were carried out in order to examine their influence on the chemistry and microstructure of the final powder. With these experiments, a cheap, reproducible, easy to implement and reliable synthesis process at room temperature has been determined. Indeed, these various characterizations indicate that the ammonium hydroxide route yields spherical, homogeneous particles whose sizes are distributed in a bimodal way. Considering the precursor from the sodium hydroxide route, which presents a bulky microstructure, with very large grains, the microstructural characteristics obtained through the ammonium hydroxide route are thus more adapted to the Cool-SPS process. Moreover, the ammonium hydroxide precursor, decomposing at lower temperature than the sodium one, provides an enhanced reactivity for subsequent sintering. The opportunity to control the microstructure of  $\text{TiO(OH)}_2$  could prove useful, not only for low temperature reactive sintering approaches, but also for catalysis applications, where microstructural parameters are determinant. Finally this precursor favors the stabilization of the anatase phase up to 1000°C, allowing the elaboration of dense anatase ceramics by Cool-SPS at 600°C.

## **Acknowledgements**

This research was supported by of DGA-AID and ICMCB laboratory. The authors would like to thank Laetitia Etienne for granulometric and TGA measurements, Alexandre Fargues for FTIR, Eric Lebraud and Stanislav Petchev for collecting the XRD data. The authors would also like to acknowledge the interns who worked on the synthesis: Mine Kocatus, Amandine Greil, Estelle Bellicini and Chloé Sanz. Michaël Josse thanks University of Bordeaux for a 6 months sabbatical leave during 2019-2020 for Cool-SPS development. Lauriane Faure thanks the AID (DGA) for funding her PhD.

## References

- [1] M. T. Sebastian, H. Wang, et H. Jantunen, Low temperature co-fired ceramics with ultra-low sintering temperature: A review, *Current Opinion in Solid State and Materials Science*, 20 (2016) 151-170
- [2] M. Nelo, J. Peräntie, T. Siponkoski, J. Juuti, et H. Jantunen, Upside-down composites: Electroceramics without sintering, *Applied Materials Today*, 15 (2019) 83-86
- [3] S. Grasso *et al.*, A review of cold sintering processes, *Advances in Applied Ceramics*, 119 (2020) 115-143
- [4] H. Guo, J. Guo, A. Baker, et C. A. Randall, Hydrothermal-Assisted Cold Sintering Process: A New Guidance for Low-Temperature Ceramic Sintering, *ACS Appl. Mater. Inter.*, 8 (2016) 20909-20915
- [5] T. Herisson de Beauvoir, A. Sangregorio, I. Cornu, C. Elissalde, et M. Josse, Cool-SPS: an opportunity for low temperature sintering of thermodynamically fragile materials, *J. Mater. Chem. C*, 6 (2018) 2229-2233
- [6] T. Hérisson de Beauvoir, F. Molinari, U. C. Chung-Seu, D. Michau, D. Denux, et M. Josse, Densification of MnSO<sub>4</sub> ceramics by Cool-SPS: Evidences for a complex sintering mechanism and magnetoelectric coupling, *Journal of the European Ceramic Society*, 38 (2018) 3867-3874
- [7] T. Herisson de Beauvoir, A. Sangregorio, I. Cornu, et M. Josse, Synthesis, sintering by Cool-SPS and characterization of A<sub>2</sub>Cu(CO<sub>3</sub>)<sub>2</sub> (A = K, Na): evidence for multiferroic and magnetoelectric cupricarbonates, *Dalton Trans.*, 49 (2020) 7820-7828
- [8] T. Herisson de Beauvoir, V. Villemot, et M. Josse, Cool-Spark plasma sintering: An opportunity for the development of molecular ceramics, *Solid State Sciences*, 102 (2020) 106171
- [9] C. Elissalde *et al.*, Single-step sintering of zirconia ceramics using hydroxide precursors and Spark Plasma Sintering below 400 °C, *Scripta Materialia*, 168 (2019) 134-138
- [10] H. Yao *et al.*, TiO(OH)<sub>2</sub> – highly effective catalysts for optimizing CO<sub>2</sub> desorption kinetics reducing CO<sub>2</sub> capture cost: A new pathway, *Scientific Reports*, 7 (2017) 2943
- [11] S. Toan *et al.*, Green, safe, fast, and inexpensive removal of CO<sub>2</sub> from aqueous KHCO<sub>3</sub> solutions using a nanostructured catalyst TiO(OH)<sub>2</sub>: A milestone toward truly low-cost CO<sub>2</sub> capture that can ease implementation of the Paris Agreement, *Nano Energy*, 53 (2018) 508-512

- [12] M. Irani, K. A. M. Gasem, B. Dutcher, et M. Fan, CO<sub>2</sub> capture using nanoporous TiO(OH)<sub>2</sub>/tetraethylenepentamine, *Fuel*, 183 (2016) 601-608
- [13] J. Ma, A.-G. Pesty, et D. Dambouret, Composé oxy-hydroxyde de titane et son procédé de fabrication, électrode et catalyseur le comprenant, (2017) WO2017/125680A1
- [14] B. Dutcher, Use of multifunctional nanoporous TiO(OH)<sub>2</sub> for catalytic NaHCO<sub>3</sub> decomposition-eventually for Na<sub>2</sub>CO<sub>3</sub>/NaHCO<sub>3</sub> based CO<sub>2</sub> separation technology, *Separation and Purification Technology*, (2011) 11
- [15] D. A. H. Hanaor et C. C. Sorrell, Review of the anatase to rutile phase transformation, *J Mater Sci*, 46 (2011) 855-874
- [16] N. Wetchakun, B. Incessungvorn, K. Wetchakun, et S. Phanichphant, Influence of calcination temperature on anatase to rutile phase transformation in TiO<sub>2</sub> nanoparticles synthesized by the modified sol-gel method, *Materials Letters*, 82 (2012) 195-198